Available online at www.sciencedirect.com
SCIENCE DIRECT
Catalysis Today 107–108 (2005) 60–67
CATALYSIS TODAY
www.elsevier.com/locate/cattod

Storage and reduction of lean–NO_x by using $H_3PW_{12}O_{40}{\cdot}6H_2O$ supported on $Ti_xZr_{1-x}O_4$

Miguel Angel Gómez-García [1,*], Veronique Pitchon, Alain Kiennemann

LMSPC, Laboratoire de Matériaux, Surfaces et Procédés pour la Catalyse, UMR 7515 du CNRS-ECPM, 25 rue Becquerel, 67087 Strasbourg Cedex 2, France

Available online 30 August 2005

Abstract

NO_x storage and reduction with $H_3PW_{12}O_{40}{\cdot}6H_2O$ (HPW) supported on $Ti_xZr_{1-x}O_4$ ($0 \leq x \leq 1$) were measured under representative lean–gas mixture conditions. Storage capacity is high (28 mg of NO_x g_{HPW}^{-1} at 170 °C) and depends on support Zr/Ti molar ratio. NO_x reduction highly depends on reducing mixture (CO, H_2 or H_2 + CO), on the presence of noble metal (platinum) and support, and on the operating conditions (long or short cycles). H_2 + CO mixture proved to be effective for NO_x reduction into N_2 even if low activity was detected for each gas separately. With short cycles of lean/rich (2/1 min) at 250 °C, (HPW-Pt)/$Ti_xZr_{1-x}O_4$ (with Zr/Ti molar ratio equal to 0.5) is significantly more active than unsupported HPW-Pt, delivering upto 40% NO_x reduction into N_2 with 75% of NO_x storage efficiency. Experimental results evidence the kinetic coupling between NO_2 reduction and CO oxidation during NO_x reduction. The combination of NO_x storage and reduction concept with a multifuctional catalyst is very promising.

Keywords: NO_x storage and reduction; Nitrogen; Tungstophosphoric acid; Titanium and zirconium mixed oxides; Platinum

1. Introduction

The interest for applying sorbent catalytic materials to NO_x (NO and NO_2) emission control has increased considerably in last years [1]. Although most of current catalytic technologies applied to NO_x catalytic decomposition are operated at temperatures higher than 300 °C, the formulation of more stringent regulations related to NO_x emissions (from mobile or stationary sources) requires of developing more efficient catalysts able to work at lower temperatures [2,3].

Previous works had demonstrated the interest of using $H_3PW_{12}O_{40}{\cdot}6H_2O$ (HPW) for NO_x storage and desorption [4]. With HPW, NO and NO_2 are stored and desorbed equimolarly without nitrate formation. The quantity of NO_x stored is large and equal to 38 mg of NO_x g_{HPW}^{-1} at 170 °C. Storage mechanism involves the substitution of HPW structural water molecules [$(H_2O)H^+(H_2O)$], by NO_x and by forming a [$(NO_2^-)H^+(NO^+)$] complex. This phenomenon is completely reversible in the presence of water at around 100 °C. However, due to the physical characteristics of HPW, its dispersion on supports is crucial for practical applications. The interest of using carbon nanotubes as support has been reported recently [5]. Nevertheless, it is required that supports must be easily disposed on a monolith and oxides supports present a high potential. Their selection has to take into account the strong acidity of HPW [6]. If a support is moderate to strongly basic (e.g., Al_2O_3, MgO), the interaction with HPW is too strong and leads to an acid–base reaction with loss of crystallinity of HPW (as detected by XRD) with a complete degradation of its storage properties. If the support is strongly acidic (e.g., SiO_2), NO_x sorption remains possible and the XRD structure of HPW exists, but the anchorage is not secured. In the case of medium acidity (e.g., ZrO_2, TiO_2 and SnO_2), the structural properties are

* Corresponding author.
E-mail address: gomezma@ecpm.u-strasbg.fr (M.A. Gómez-García).
[1] On leave from Departamento de Ingeniería Química, Universidad Nacional de Colombia, Sede Manizales, Colombia.

0920-5861/$ – see front matter © 2005 Elsevier B.V. All rights reserved.
doi:10.1016/j.cattod.2005.07.164

retained (XRD) and the storage capacity remains high. Consequently, oxides supports can be selected from their isoelectric point (around 7). From those results, and in order to improve the performance of the simple titanium and zirconium oxides, we had chosen $Ti_xZr_{1-x}O_4$ materials as support for HPW. These materials are also able to store NO_x as reported in the literature [7]. The catalytic system is completed by including a noble metal (1 wt.% Pt) which role will be that of activating reductant agent.

The objective of this study is to develop a catalyst for NO_x abatement by using NO_x storage then reduction into nitrogen. This catalytic system integrates the NO_x storage properties of HPW, the support properties for NO_x adsorption and the noble metals performance for NO_x dissociation and reductant activation.

2. Experimental

2.1. Supports

TiO_2 and ZrO_2 oxides and several $Ti_xZr_{1-x}O_4$ mixed oxides (Zr/Ti molar ratio = 0.25, 0.5, 1 and 2) were prepared from zirconium (IV) *n*-propoxide (70% propanol) ($C_{12}H_{28}O_4Zr$, Fluka) and titanium (IV) *i*-propoxide (98%) ($C_{12}H_{28}O_4Ti$, Strem) by forming an alcoholic solution (1M propanol) and by mixing with an excess of water [8,9]. The obtained mixture was filtered, washed, dried and calcined at 750 °C for 4 h.

2.2. Catalysts preparation and characterisation

The impregnation of the supports was carried as follows: 12-tungstophosphoric acid hexahydrate (HPW) was dried overnight at 120 °C in order to obtain $H_3PW_{12}O_{40}{\cdot}6H_2O$. A specific amount of dried HPW was dissolved in water in order to obtain a 0.01 M solution. The addition of platinum into this HPW solution was made by using a precise amount of platinum precursor (H_2PtCl_6). HPW or HPW-Pt solutions were added drop wise to calculated amount of support, which was previously dispersed into water [10,11]. Supported catalysts comprise HPW and Pt loadings of 20–65 and 1 wt.%, respectively. Suspension was stirred in a glass vessel, and slowly evaporated until dryness. Subsequently, the solid was ground to fine particles and dried.

Catalysts were characterised before and after catalytic test by using several techniques. Specific surface area (S_{BET}) was determined by N_2 adsorption in a Coulter SA 3100 at 77 K, using a sample of approximately 500 mg. SEM analyses were performed on a JEOL-JSM 840 microscope. Cathode environment was operated at 10^{-3} Pa. Samples were fixed on a support with a carbon scotch. Before analyzing, a gold monolayer was deposited on samples in order to improve its electric conductivity. X-ray diffraction (XRD) was performed with a Siemens D-5000 diffractometer using the Cu Kα radiation, with a continuous acquisition between 5° and 80°, a step of 0.02° and a step time of 10 s. For Fourier transform infrared spectroscopy (IR) studies, a fraction of the catalyst was diluted into KBr and pressed in the form of a pellet. The same mass of KBr and sample were used for all the solids and the IR spectra reported results from a previous subtraction of the blank. IR spectra were recorded using a Nicolet 5DXC and the spectral domain was between 400 and 4000 cm^{-1} with a 2 cm^{-1} resolution. XPS spectra were recorded on a ThermoVG (Multilab 2000) spectrometer at room temperature, under a vacuum of 10^{-8} Pa. Al Kα radiation ($h\nu$ = 1486.6 eV), obtained by bombarding the Al anode with an electron gun operating at a beam current of 15 mA and an accelerating voltage of 15 kV, was used.

2.3. Test procedures

2.3.1. Apparatus and gas composition

The experimental set up, a full computer driven reactor system, was constructed for including powdered laboratory-scale catalysts. The experiments were conducted in a flow reactor using a series of mass flow controllers by alternating simulated lean gas compositions with different times of excursion. After mass flow meters, gas mixture is homogenised before going to the reaction section. Saturators allow us to reach the defined water content in gas mixtures (only air and/or helium will go through saturators).

The tests were made using a lean (NO = NO_2 = 500 ppm, O_2 = 10%, CO_2 = 5%, H_2O = 5% and He as a balance) and rich (H_2 = 1% or CO = 3% or H_2 = 1% + CO = 2%; with H_2O = 5% and He as a balance) gas mixtures. The modified gas lean mixture is related with an oxidation catalyst previous to the NO_x storage system. With that catalyst, hydrocarbons and CO are oxidised into CO_2 and NO is partly transformed into NO_2. Thus, the NO/NO_2 ratio used was fixed taking into account the oxidation catalyst performance and NO–NO_2 thermodynamic equilibrium. Additionally, it was pointed out that the presence or absence of hydrocarbons does not influence NO_x storage capacity of HPW [4]. After reduction, an additional excursion of wet air (H_2O = 5%) through the catalyst was made with the aim of evaluating the presence of residual NO_x stored.

Formed mixtures are introduced into the reactor which is a 1 cm quartz diameter with 300 mg of catalyst and a flow of 300 ml min^{-1} (GSHV ≈ 20,000 h^{-1}). NO and NO_2 concentrations were monitored by NO and NO_2 analysers (Binos Rosemount Analytical) over a range of 0–3000 ppm (±10 ppm). It is necessary to remove the water because of its interference on chromatography and IR analysis. In such way, dry air is fed in counter-current to the shield of two permeation tubes (serie Perma Pure Inc.), composed by a Nafion® membrane which is permeable to water molecules. Analytical instruments also include a gas phase μ-chromatograph (Agilent 3000, equipped with a molecular

sieve column (5 Å) and a thermal conductivity detector (TCD)) and a quadrupole mass spectrometer (HPR-20, Hiden Analytical).

2.3.2. Standard test procedure

NO_x storage and desorption were made isothermally at a selected value between 170 and 400 °C. The isothermal standard procedure comprised a stabilisation period, for the complete fuel-lean gas mixture, by the bypass, at the same time as reactor is heated to selected temperature, with a ramp rate of 4 °C min^{-1}. Succeeding, system is stabilised at these last conditions for 15 min. Subsequently, fuel-lean gas mixture is changed from by-pass to reactor. NO_x storage manifests itself by the drop of NO and NO_2 concentration signals. At the end of storage sequence, the original concentration of NO_x is reached finalising storage period. Reduction or desorption begin with a very fast change from lean to rich gas mixture and/or wet air at constant temperature. The amount of NO_x stored and then released upon desorption was estimated by an integration of the curve below or above the baseline for absorption or desorption, respectively, and by expression as mg or moles of NO_x g^{-1}_{HPW} (with NO_x calculated from the average molar weight between NO and NO_2). The NO_x reduction percentage was calculated as: (total nitrogen stored − total nitrogen desorbed)/(total nitrogen stored) × 100, in accordance with μGC, mass spectrometer and NO_x analysers results.

3. Results

3.1. Catalysts characterisation

3.1.1. Support textural and morphological characterisation

Mixed oxides present higher specific surface than those of simple oxides. Their values were 14, 25, 35, 38, 32 and 19 m^2 g^{-1} for TiO_2; Zr/Ti = 0.25, 0.5, 1, 2; and ZrO_2, respectively. For mixed oxide supports, pore size distribution is more evenly distributed around 12–20 nm.

From SEM results for TiO_2 and Zr–Ti materials, the size and aspect of particles suggest the presence of aggregates of spherical grains of dimension <1 μm with the existence of porosity in the submicrometer range. For ZrO_2, SEM analysis confirmed a low degree of surface roughness with no obvious structure evident at 1 μm magnification.

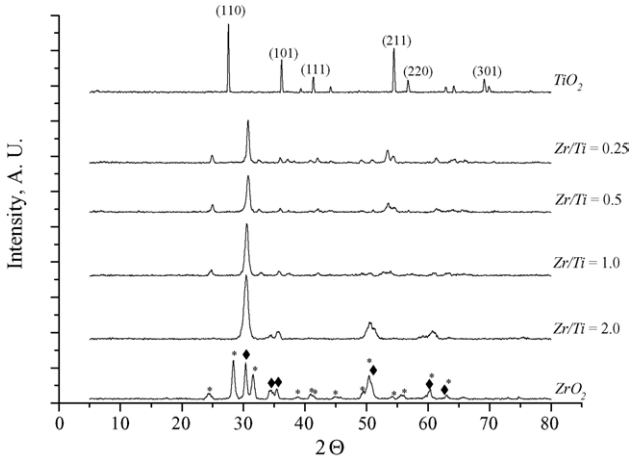

Fig. 1. XRD patterns of $Ti_xZr_{1-x}O_4$ ($0 \leq x \leq 1$) catalyst calcined at 750 °C: (◆) tetragonal zirconia and (*) monoclinic zirconia.

3.1.2. Support crystalline characterisation

Crystalline phases were identified from XRD studies by comparison with the JCPDS corresponding files. Fig. 1 shows the results for the catalysts prepared at 750 °C.

It could be seen that XRD patterns of ZrO_2 correspond to that of a mixture of tetragonal and monoclinic (baddeleyite) structure (JCPDS file: 37–1484) and those of TiO_2 correspond to that of rutile structure (JCPDS file: 78–1510) [12]. Mixed oxides are characterised by the presence of a large and wide diffraction peaks. This broadening could be ascribed to the distortion of ZrO_2 crystal structure due to the incorporation of new metal elements. Actually, the formation of a solid solution could be considered for diluted samples from which it is possible to say that X-ray diffraction patterns are dominated by the ZrO_2 patterns (the incorporation of Ti into ZrO_2 matrix). For Zr/Ti molar ratio between 0.5 and 1 the samples crystallize in the orthorhombic srilankite structure [13].

3.1.3. Support surface composition characterisation

Zr–Ti based materials were additionally characterised by XPS. The Zr 3d level splitting is well defined: the Zr $3d_{5/2}$ signals are at 183.2 and 185.6 eV, in good agreement with other works in the literature [14]. In the case of titanium, the Ti $2p_{3/2}$ level splitting is also well defined at 459.6 and 465.4 eV. XPS results are summarised in Table 1 and compared to the theoretical Zr/Ti molar ratio and elemental analysis (EA) results.

Table 1
Comparison of Zr/Ti ratio obtained by XPS to theoretical and to elemental analysis values

Zr/Ti theoretical	Zr/Ti Exp, XPS	Zr/Ti Exp, EA	O 1s BE (eV)	Zr $3d_{5/2}$ BE (eV)	Ti $2p_{3/2}$ BE (eV)
0.5	0.42	0.51	531.0	183.2–185.6	459.7–465.4
1.0	1.30	1.02	531.6	183.8–186.2	459.9–465.6
2.0	2.90	2.04	531.3	183.4–185.8	459.6–465.3

Binding energy (BE) of Zr $3d_{5/2}$ Ti $2p_{3/2}$. The charge correction was made considering that the C 1s signal was centred at 284.8 eV.

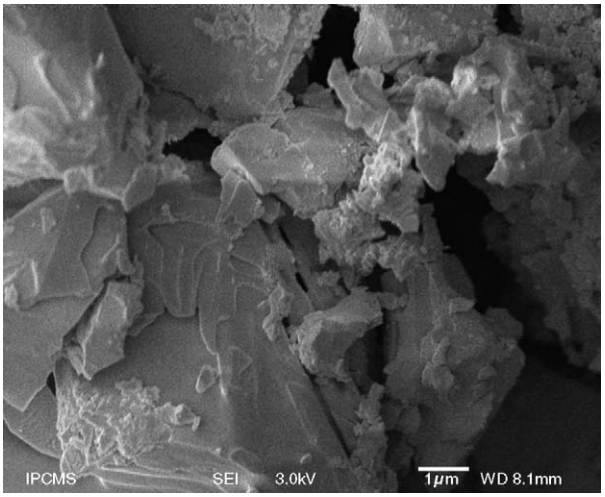

Fig. 2. SEM micrography of 65% HPW/(Zr/Ti = 0.5) catalyst.

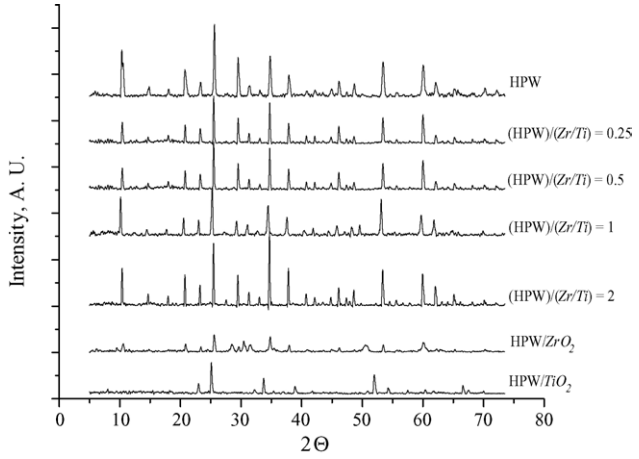

Fig. 3. XRD patterns of HPW deposited on $Ti_xZr_{1-x}O_4$ ($0 \leq x \leq 1$) supports calcinated at 750 °C ($R = 1.86\%_{HPW}$ g m^{-2}).

There is a little shift, in parallel directions, of O 1s and Zr $3d_{5/2}$ and Ti $2p_{3/2}$ lines positions, although the correspondence difference in binding energy values is close to the precision limits of XPS measurements (0.5 eV). Another feature is the variable content of superficial Zr/Ti ratio, which presents a deviation respect to the theoretical value: the higher the Zr content the higher the Zr/Ti molar ratio in the surface.

3.2. HPW impregnation on $Zr_xTi_{1-x}O_4$

The presence of supported HPW is revealed from SEM results as the existence of well ordered flat layers like aggregates on a support matrix (Fig. 2). Support was easily identifiable by SEM even at high HPW loads. For impregnating HPW, the starting point was to define the quantity of HPW supported necessary to preserve the crystal phase of HPW. The presence of important HPW loading is justified since the NO_x storage in HPW is a bulk phenomenon [15]. A previous work in our laboratory was made in order to find the more suitable conditions for the system HPW/TiO_2 [16]. It was concluded that

- The optimal loading of HPW is around 50% when the support has a specific surface in the range 20 to 80 m^2 g^{-1}. Consequently, we made the impregnation on TiO_2, ZrO_2 and $Ti_xZr_{1-x}O_4$ taking as reference the parameter R, which is the ratio between HPW loading percentage per unit of specific surface.
- It was also defined that the 50% HPW loading is equivalent to 4–5 HPW monolayers available for NO_x storage. At this condition, the parameter R must have a value of $1.86\%_{HPW}$ g m^{-2}.

Fig. 3 shows XRD results for all catalysts. It could be seen that well-defined HPW phase can be obtained over $Ti_xZr_{1-x}O_4$ catalysts at $R = 1.86\%_{HPW}$ g m^{-2} (equivalent to, for example, $65\%_{HPW}$ for Zr/Ti = 0.5 support). For simple oxides, support structure was also detectable after impregnating HPW.

3.3. NO_x storage with HPW supported on $Ti_xZr_{1-x}O_4$

NO_x storage with HPW/$Ti_xZr_{1-x}O_4$ series of catalysts was evaluated under representative exhaust lean gas mixture. The quantity of NO_x stored was higher when using mixed oxides than simple oxides as supports (Fig. 4) with the presence of a maximum at intermediate compositions ($0.5 < Zr/Ti < 2$). For mixed Zr–Ti oxides, the storage capacity was of around 28 of NO_x g^{-1}_{HPW} at 170 °C compared to 38 of NO_x g^{-1}_{HPW} for bulk HPW. In fact, after impregnating, part of HPW (''a first layer'') is utilised to anchoring HPW to support structure and that part lost its structure and storage properties (acid–base reaction). Subsequent HPW layers will keep their NO_x storage properties. The process of storage-desorption is reproducible over several runs. Desorption peaks for supported catalysts are wider and shorter than that of HPW

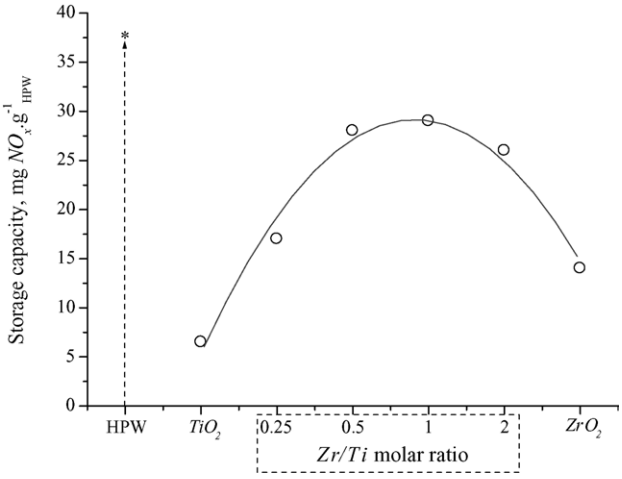

Fig. 4. Influence of HPW supported percentage on Zr/Ti = 0.5 at 170 °C.

needing longer times the earlier for completing NO_x desorption.

The amount of NO_x trapped and released and the maximum temperature of operation are some of the key parameters for HPW practical applications. Therefore, besides storage capacity and for comparing catalysts performance, it is also necessary to define another parameter to quantify the storage efficiency: this is a representation of NO_x absorption rate. Consequently, we have defined the storage efficiency as a function of the quantity of NO_x stored over 1 min according to

$$\text{storage efficiency}\,(\%) = \frac{\int_{1\,\text{min}}[NO_x]_{\text{stored}} \times \text{dt}}{\int_{1\,\text{min}}[NO_x]_{\text{fed}} \times \text{dt}} \times 100$$

In many cases, storage efficiency is a more representative parameter for NO_x traps applications than storage capacity.

3.3.1. Influence of HPW loading and temperature upon NO_x storage and efficiency

From above results, Zr/Ti = 0.5 was kept for evaluating the influence of HPW loading and temperature upon NO_x storage. For this support, we verified that HPW structure could be retained from ~20%$_{HPW}$ loading. However, NO_x storage capacity and efficiency present a high dependence on the percentage of HPW loading (due principally to the bulk mechanism that governs this process). At 170 °C, from 20 to 65 wt.% of HPW loading, the storage efficiency increases from 25 to 60% and the storage capacity from 8 to 28 mg $NO_x\,g^{-1}_{HPW}$, respectively.

Additional storage tests were performed isothermally at various temperatures between 200 and 400 °C for 65 wt.% HPW ($R = 1.86\%_{HPW}\,g\,m^{-2}$) deposited on Zr/Ti = 0.5 (Fig. 5). We have verified, by XRD and IR, that HPW structure is preserved after each test.

Temperature range between 170 and 200 °C allows obtaining the best NO_x storage capacity and efficiency. The efficiency and the amount of NO_x absorbed remain high up to 250 °C for supported HPW and they are comparable to that of HPW alone. Between 250 and 300 °C, HPW storage capacity and efficiency decrease rapidly. However, for supported HPW that lost in the storage performance is more steadily, evidencing the relevance of support. At 400 °C storage is no longer obtained. Comparable results were obtained when using supported HPW-Pt.

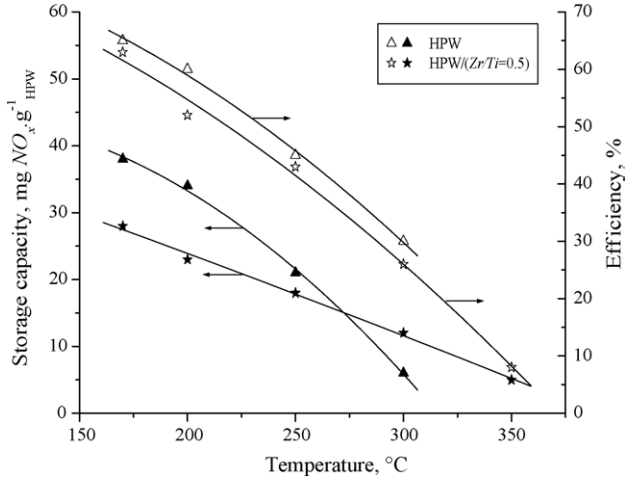

Fig. 5. Temperature influence upon NO_x storage capacity and efficiency of HPW and 65 wt.% HPW deposited on Zr/Ti = 0.5.

Since similar values of NO_x storage capacity and efficiency where detected for HPW and supported HPW at 250 °C, we kept this temperature for studying NO_x storage and reduction.

3.4. NO_x storage and reduction

3.4.1. HPW

The nature and quantity of reduction products strongly depend on desorbing/reductant mixture as presented in Fig. 6. In this figure, NO_x storage is manifested from the drop of NO and NO_2 signals and is equal to 0.63 mmol $NO_x\,g^{-1}_{HPW}$ for all examples given.

Thermal desorption in presence of wet air generates a simultaneous and equimolar desorption of NO and NO_2 during both procedures: isothermal (0.39 mmol $NO_x\,g^{-1}_{HPW}$) and cooling (0.24 mmol $NO_x\,g^{-1}_{HPW}$) (Fig. 6a). The molar balance confirms that all NO_x absorbed was desorbed.

The presence of reducing agent modifies completely the NO_x desorption mode when comparing to that of using wet air. In fact, when using only 1% H_2 as reductant (1% H_2, 5% H_2O and helium as balance), a slow isothermal desorption of 0.32 mmol $NO_x\,g^{-1}_{HPW}$ is detected (Fig. 6b). This desorption is mostly as NO. An additional sequence, under wet air and by decreasing the temperature until 80 °C, allows desorbing simultaneous and equimolarly the remaining NO and NO_2 (0.28 mmol $NO_x\,g^{-1}_{HPW}$).

When using 3% CO for reducing (Fig. 6c), a slow isothermal desorption of a mixture of NO and NO_2 ($NO/NO_2 \sim 2$) is observed (0.35 mmol $NO_x\,g^{-1}_{HPW}$). Again, after switching to wet air mixture, the characteristic HPW equimolar desorption of NO and NO_2 is observed (0.27 mmol $NO_x\,g^{-1}_{HPW}$).

Nevertheless, when replacing partially CO by H_2, whilst keeping the total reductant concentration constant, 2% CO and 1% H_2, a desorption of 0.42 mmol of $NO_x\,g^{-1}_{HPW}$ was detected (Fig. 6d). It seems that hydrogen improves NO_x desorption quantity and rate. Once more, NO_x desorption is completed with an additional sequence under wet air and by decreasing the temperature until 80 °C: as expected, an equimolar desorption of NO and NO_2 was detected (0.20 mmol $NO_x\,g^{-1}_{HPW}$).

After each test showed in Fig. 6, the molar balance between NO_x stored and desorbed (isothermally and by cooling) corresponds accurately. The storage efficiency has an average value of 48%. In any case, neither N_2O nor NH_3 formation were detected.

NO_x reduction with HPW and by using CO, H_2 or their combination has demonstrated to be a very slow process.

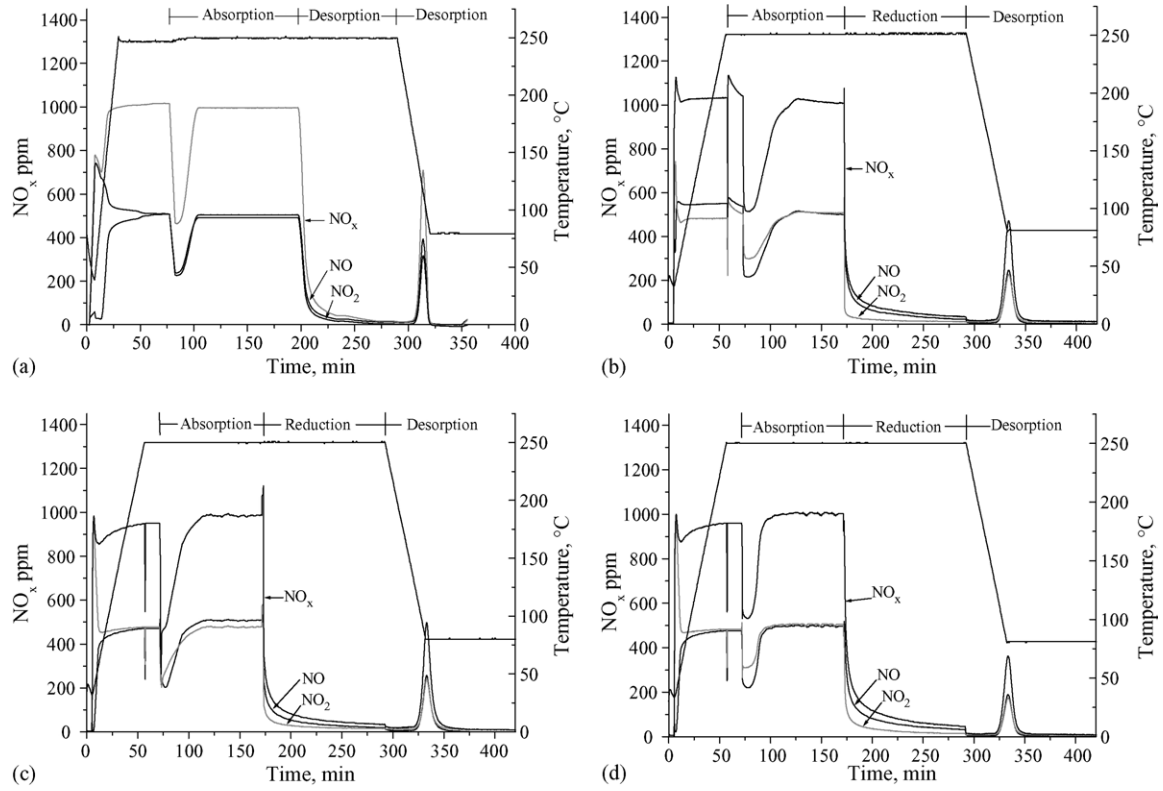

Fig. 6. Evolution of stored NO_x with HPW after passage to: (a) wet air, (b) 1% H2, (c) 3% CO and (d) 1% H_2 + 2% CO at 250 °C; followed by a desorption sequence under wet air (down to 80 °C).

NO_2 is only partially reduced into NO but not into nitrogen. In fact, even the use of long exposition time to rich mixtures was not enough for both the complete regeneration of occupied sites by NO_x in HPW and the NO_x reduction. Consequently, we decide to include the presence of a noble metal with the purpose of activating reductive agent.

3.4.2. HPW-Pt

The addition of Pt affects strongly the chemical behaviour occurring during the course of rich operation. NO_x desorption observed at the beginning of the rich phase is strongly accelerated and it is desorbed mainly as NO (reaching values higher than 5000 ppm).

With HPW-Pt, when using H_2 for reducing, the amount of NO_x stored corresponds to that of NO desorbed. In the case of CO as reductive agent, CO_2 formation was detected in addition to an accelerated and concomitant desorption of NO. In fact, NO comes from both: the desorption from $[(NO^+)H^+(NO_2^-)]$ complex (in HPW structure) and from NO_2 reduction. The coincidence of CO_2 and NO maxima implies the existence of a kinetic coupling between both CO oxidation and NO_2 reduction phenomena. Additionally, with CO, a difference <10% between NO_x stored and desorbed was detected. Neither N_2O nor NH_3 formation were detected by mass spectrometry (additionally, no HPW structural changes were observed by XRD). N_2 evolution was roughly detected by μGC (very fast desorption peak).

After replacing partially CO by H_2 (by using 2 and 1%, respectively), while preserving total reductant concentration (3%), we observe that the difference between NO_x storage and desorption is of ∼13%. A number of studies have reported evidence for hydrogen-assisted NO dissociation on supported platinum [17,18]. For our catalytic system, an H_2 assisted mechanism could be also suggested due to the ability of hydrogen to reduce metals and the role of these metals in the reduction process under analysis. Although N_2O or N_2 formation could be facilitated from NO dissociation, the former was never detected.

3.4.3. (HPW-Pt)/(Zr/Ti = 0.5)

After supporting HPW-Pt on Zr/Ti = 0.5, we observe a marked difference between amount of NO_x stored and desorbed, with a more clear detection of nitrogen, highly dependent on rich mixture: 4, 16 and 26% when using 1% H_2, 3% CO and 1% H_2 + 2% CO, respectively. Again, and now more evident, an H_2 assisted mechanism could be proposed. Once more, neither N_2O nor NH_3 formation are detected. The storage efficiency remains important at environ 52%. These results evidenced the crucial role of support in this system.

3.5. NO_x storage and reduction cycles

NO_x storage and reduction (NSR) concept includes cycles of switching between lean and rich mixtures [19].

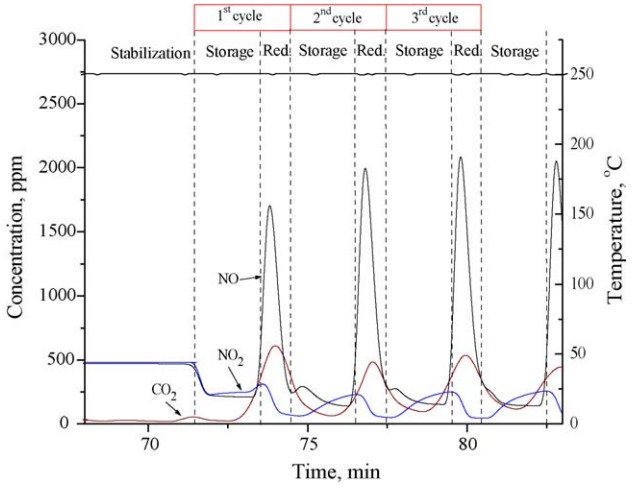

Fig. 7. HPW-Pt behaviour during cycles of lean (2 min) and rich (1 min: 2% CO and 1% H_2) operation at 250 °C.

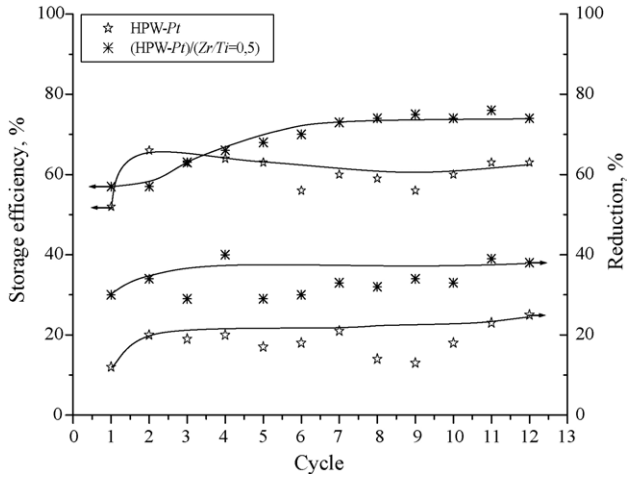

Fig. 8. NO_x storage efficiency and reduction percentage with HPW-Pt and (HPW-Pt)/(Zr/Ti = 0.5) during 12 cycles lean (2 min) and rich (1 min: 2% CO and 1% H_2) at 250 °C.

Since total system efficiency has maximum if storage process is optimum [20], it is not necessary to saturate NO_x sorbent material but to operate at conditions where the highest quantity of gas is stored in the shortest time. As consequence, NO_x treatment cycle was modified to have 120 s for lean and 60 s for rich. An example of the evolution of those experiments is presented in Fig. 7 for HPW-Pt when using 2% CO + 1% H_2 wet mixture for reducing.

NO_x storage-reduction cycles (12 cycles) are perfectly reproducible which proves the continuous regeneration of NO_x storage sites by rich mixture of gases. With HPW-Pt, an average uptake of 0.51 mmol of NO_x g_{HPW}^{-1} during 2 min of lean phase, with an efficiency of 63%, was detected. After switching to rich mixture, a fast NO desorption give rise to a sharp peak in concomitance with a peak of CO_2 formation and to NO_2 consumption. The desorption represents 0.39 mmol of NO_x g_{HPW}^{-1} and 0.03 mmol of NO_x g_{HPW}^{-1}, with the formation of 0.18 mmol of CO_2 g_{HPW}^{-1}. The ratio NO/$CO_2 \approx 2$ confirms the kinetic coupling between NO_2 reduction and CO oxidation. A final additional sequence, by decreasing the temperature until 80 °C, allows us to verify that there is not NO_x remaining in HPW structure. This meaning that 20% of NO_x was reduced into N_2. NO_x reduction percentage and storage efficiency are highly improved during short cycles operation with respect of long cycles (described previously in Fig. 6). Results are summarised Fig. 8 for both supported and unsupported HPW-Pt.

After 12 cycles, the average performance of supported catalyst improves from 20 to 38% for NO_x reduction into N_2 and from 60 to 75% for storage efficiency, when comparing with unsupported HPW-Pt. The comparison of supported HPW-Pt performance, after long and short cycles (as presented in Fig. 6), reveals that NO_x reduction and efficiency percentage was improved from ~13 to 40% and from 52 to 75%, respectively. These facts evidence the crucial role of both support and short cycle operation mode.

3.6. Reduction mechanism

From the experimental evidence presented above it seems that the mechanism for NO_x reduction into N_2 with (HPW-Pt)/(Zr/Ti = 0.5) catalyst, when using CO and H_2, involves the following events:

- After switching from lean (NO_x storage period) to rich wet mixtures, NO and NO_2 are released from the bulk of HPW after exchanging with water (regenerating HPW structure).
- The reduction of Pt particles and support, by H_2, generates Pt^0 and M^+ (support) active sites. Metal particles can be related with both the support and/or HPW. In fact, It is also possible to consider the presence of another different type of active site (cationic) formed by the interaction between Pt and the proton of HPW structure: Pt–$H^{\delta+}$ [21].
- Adsorption of H_2 and/or CO on Pt active sites (it is also possible to consider the formation of formyl type species: $C_xH_yO_z$ [22]).
- Adsorption of NO_2 (previously released from HPW) on Pt^0 active sites oxidizing metal sites and releasing NO. Part of formed NO could be also dissociated over cationic sites into nitrogen (which is released) generating adsorbed oxygen, which reacts with CO (or formyl type species) forming CO_2. In fact, from the concomitant evolution of NO and CO_2, it could also be claimed the existence of a kinetic coupling between the dissociation of NO with N_2 and CO_2 formation (the scavenging of adsorbed oxygen species left after NO dissociation, and restoring the active sites [23]). In fact, in a catalytic sequence for CO/NO reaction over (HPW-Pt)/(Zr/Ti = 0.5), the whole reaction does not take place on a unique site nor the two reactants are in competition [24].
- Hydrogen assists the reduction process by generating Pt active sites (by scavenging the adsorbed oxygen which has been left by oxygen adsorption (lean mixture) or NO dissociation with H_2O formation).

4. Conclusions

The interest of using $Ti_xZr_{1-x}O_4$ as support for HPW-Pt in the catalytic depollution of NO_x has been demonstrated. This study includes the application of a new concept for lean NO_x reduction, which involves a ''multifunctional catalyst'': a catalytic material having integrated structures of NO_x sorbing sites and catalytically active sites for reducing. The successive use of short lean/rich periods, implying NO_x storage/fast desorption-reduction, is a very promising concept. In fact, supported catalyst is able to trap NO_x with high efficiency (∼75%), to desorb them very quickly when switching upon rich mixture and reducing them in an extent of ∼40% at 250 °C with 2% CO + 1% H_2 wet mixture. It could be suggested that the reduction process includes the presence, at least, of two different active sites: reduced metal particles (Pt^0) and another site formed by the interaction between Pt and the proton of HPW structure (Pt–$H^{\delta+}$). NO_x reduction process is highly improved by the assistance of hydrogen for regenerating active sites.

Acknowledgement

ADEME (Agence de l 'Environnement et de la Maîtrise de l 'Energie, France) is greatly acknowledged for financial support.

References

[1] R. Burch, J.P. Breen, F.C. Meunier, Appl. Catal. B: Environ. 39 (2002) 283.
[2] J.W. Erisman, P. Grennfelt, M. Sutton, Environ. Int. 29 (2003) 311.
[3] B. Ramachandran, R.G. Hermann, S. Choi, H.G. Stenger, C.E. Lyman, J.W. Sale, Catal. Today 55 (2000) 281.
[4] S. Hodjati, C. Petit, V. Pitchon, A. Kiennemann, J. Catal. 197 (2001) 324.
[5] M.A. Gómez-García, V. Pitchon, A. Kiennemann, M. Corrias, Ph. Kalck, Ph. Serp, Topics Catal. 30/31 (2004) 335.
[6] S. Hodjati, K. Vaezzadeh, C. Petit, V. Pitchon, A. Kiennemann, Topics Catal. 16 (2001) 151.
[7] M. Machida, S. Ikeda, D. Kurogi, T. Kijima, Appl. Catal. B: Environ. 35 (2001) 107.
[8] M.P. Feth, J. Non-Cryst. Solids 298 (2002) 43.
[9] R. Merkle, H. Bertagnolli, J. Math. Chem. 8 (1998) 2433.
[10] I.V. Kozhevnikov, A. Sinnema, R.J.J. Jansen, K. Pamin, H. van Bekkum, Catal. Lett. 30 (1995) 241.
[11] F. Marme, G. Coudurier, J.C. Védrine, Micropor. Mesopor. Mater. 22 (1998) 151.
[12] K. Otsuka, Y. Wang, M. Nakamura, Appl. Catal. A: Gen. 183 (1999) 317.
[13] R. Merkle, H. Bertagnolli, J. Math. Chem. 8 (1998) 2433.
[14] J.F. Moulder, W.F. Sticle, P.E. Sobol, K.D. Bomben, in: J. Chatain (Ed.), Handbook of XPS, Perkin-Elmer Corporation, Wellesley, MA, 1992.
[15] T. Okuhara, N. Mizuno, M. Misono, Adv. Catal. 41 (1996) 113.
[16] S. Thomas, K. Vaezzadeh, V. Pitchon, Topics Catal. 30/31 (2004) 207.
[17] R. Burch, T.C. Watling, Catal. Lett. 37 (1996) 51.
[18] N. Macleod, R.M. Lambert, Appl. Catal. B: Environ. 35 (2002) 269.
[19] N. Takahasi, H. Shinjoh, T. Ijima, T. Suzuki, K. Yamakazi, K. Yokota, H. Suzuki, S. Miyoshi, S. Matsumoto, T. Tanizawa, T. Tanaka, S. Tateishi, K. Kasahara, in: Proceedings of the First International Congress Environmental Catalysis, Pisa, 1995, p. 45.
[20] A. Kiennemann, J.A. Martens, B. Kasemo, E. Chaize, D. Webster, B. Krutzsch, G. Wenninger, M. Weibel, P. Stapf, A. Funk, SAE, No. 982592, 1998.
[21] A.V. Ivanov, T.S. Vasina, V.D. Nissenbaum, L.M. Kustov, M.N. Timofeeva, J.I. Houzvicka, Appl. Catal. A: Gen. 259 (2004) 65.
[22] J.P. Hindermann, G.J. Hutchings, A. Kiennemann, Catal. Rev. Sci. Eng. 35 (1993) 193.
[23] I. Manuel, C. Thomas, C. Bourgeois, H. Colas, N. Matthess, G. Djéga-Mariadassou, Catal. Lett. 77 (2001) 193.
[24] G. Djéga-Mariadassou, F. Fajardie, J.F. Tempère, J.M. Manoli, O. Touret, G. Blanchard, J. Mol. Catal. A 161 (2000) 179.